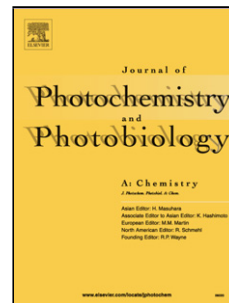


## Accepted Manuscript

Title: Preparation and characterization of Fe<sub>3</sub>O<sub>4</sub>/SiO<sub>2</sub>/CdS nanocomposites as efficient magnetic photocatalysts for the reduction of nitro compounds under visible LED irradiation

Authors: Parvin Eskandari, Foad Kazemi



PII: S1010-6030(18)30154-0  
DOI: <https://doi.org/10.1016/j.jphotochem.2018.06.011>  
Reference: JPC 11328

To appear in: *Journal of Photochemistry and Photobiology A: Chemistry*

Received date: 4-2-2018  
Revised date: 3-6-2018  
Accepted date: 4-6-2018

Please cite this article as: Eskandari P, Kazemi F, Preparation and characterization of Fe<sub>3</sub>O<sub>4</sub>/SiO<sub>2</sub>/CdS nanocomposites as efficient magnetic photocatalysts for the reduction of nitro compounds under visible LED irradiation, *Journal of Photochemistry and Photobiology, A: Chemistry* (2018), <https://doi.org/10.1016/j.jphotochem.2018.06.011>

This is a PDF file of an unedited manuscript that has been accepted for publication. As a service to our customers we are providing this early version of the manuscript. The manuscript will undergo copyediting, typesetting, and review of the resulting proof before it is published in its final form. Please note that during the production process errors may be discovered which could affect the content, and all legal disclaimers that apply to the journal pertain.

# Preparation and characterization of $\text{Fe}_3\text{O}_4/\text{SiO}_2/\text{CdS}$ nanocomposites as efficient magnetic photocatalysts for the reduction of nitro compounds under visible LED irradiation

Parvin Eskandari<sup>a</sup>, Foad Kazemi<sup>b,c\*</sup>

<sup>a</sup> Department of Chemistry, Zanjan Branch, Islamic Azad University, 49195-467, Zanjan, Iran

<sup>b</sup> Department of Chemistry, Institute for Advanced Studies in Basic Sciences (IASBS), Gava Zang, 49195-1159, Zanjan, Iran

<sup>c</sup> Center for Climate and Global Warming (CCGW), Institute for Advanced Studies in Basic Sciences (IASBS), Gava Zang, 45137-66731, Zanjan, Iran

Tel: 33153219

Fax: 33153232

Email: kazemi\_f@iasbs.ac.ir

## Graphical Abstract



## Highlights

- $\text{Fe}_3\text{O}_4/\text{SiO}_2/\text{CdS}$  photocatalysts were synthesized through a facile and convenient method.
- The photocatalytic reduction of aromatic nitro compounds to their corresponding amines was achieved under blue LED (3W) irradiation.
- $\text{Fe}_3\text{O}_4/\text{SiO}_2/\text{CdS}$  nanocomposite had higher photocatalytic activity than bare CdS and commercial CdS (Aldrich).
- The magnetic photocatalyst could be recovered easily using an external magnetic field and reused three times.

### Abstract:

A series of magnetic  $\text{Fe}_3\text{O}_4/\text{SiO}_2/\text{CdS}$  nanocomposites were synthesized through a facile and convenient method. The characterization of the prepared nanocomposites was performed by Fourier transform infrared spectroscopy (FT-IR), X-ray diffraction (XRD), scanning electron microscopy (SEM), transmission electron microscopy (TEM), energy dispersive X-ray (EDX), vibrating sample magnetometer (VSM), UV-Vis spectroscopy, and UV-Vis diffuse reflectance spectroscopy (DRS). The prepared magnetic photocatalysts were first utilized for the photocatalytic reduction of nitro compounds under visible LED irradiation. The  $\text{Fe}_3\text{O}_4/\text{SiO}_2/\text{CdS}$  nanocomposites exhibited enhanced photoactivity compared with the bare CdS and commercial CdS (Aldrich). The results demonstrated that  $\text{Fe}_3\text{O}_4/\text{SiO}_2/\text{CdS}$  nanocomposites have potential to provide a promising visible light driven photocatalyst for the selective reduction of nitro compounds to corresponding amines under mild conditions. The prepared photocatalyst can be recovered by magnetic separation and successfully reused for 3 cycles.

**Keywords:** Photocatalysis, Magnetic CdS nanocomposite, Aromatic nitro compounds, LED irradiation

### 1. Introduction:

Semiconductor photocatalysis has been gaining increasing attention as the most promising potential for solar energy conversion and environmental remediation [1-6]. Among various semiconductor photocatalysts, cadmium sulfide (CdS), owing to its suitable band gap (2.4 eV), corresponds well to the spectrum of sunlight [7]; and for its size-

dependent electronic and optical properties [8] is being considered for the wide range of applications including solar cells [9-11], biosensors [12], field-effect transistors (FET) [13], and as a photocatalyst [14-18]. In order to control the size, stabilize, and enhance the visible light activity of semiconductors nanocrystals, numerous papers describe the deposition and immobilization of nanoparticles on inert materials, such as silica [15], carbon [16, 17], graphene [5, 18-21], zeolites [22], and other mesoporous matrices [23]. Among various supporting materials, magnetically separable nanoparticles have been intensively studied because of their unique properties to facilitate the separation of photocatalyst from the reaction mixture by simply applying an external magnetic field [24-27]. Recently, some groups have achieved delightful success in this area; for example, Liu and co-workers have synthesized  $\text{Fe}_3\text{O}_4/\text{CdS}$  nanocomposites that exhibited both fluorescence and photocatalytic activity toward the decomposition of methyl orange in aqueous solution [14]. Hu and co-workers have synthesized one-dimensional (1D)  $\text{Fe}_3\text{O}_4/\text{C}/\text{CdS}$  coaxial nanochains as highly efficient and recyclable photocatalysts for water treatment [16].  $\text{Fe}_3\text{O}_4$ -doped CdS hollow sphere has been synthesized by combining  $\text{Fe}_3\text{O}_4$  with nanoparticulate CdS and applied as a photocatalyst in the degradation of organic dyes [27]. Moreover,  $\text{TiO}_2$  based magnetic photocatalysts have been enjoying great research interest for their potential in photocatalysis [28-32]. In addition, some novel magnetic photocatalytic nanoreactors [33, 34] and a novel magnetic intercalation  $\text{Fe}_3\text{O}_4\text{-QDs}@g\text{-C}_3\text{N}_4/\text{ATP}$  photocatalyst have been developed more recently by Zhu et al. [35]. However, the methods in which they have been utilized often involve photocatalytic degradation of pollutants and water treatment [36-38]. Notably, the photocatalytic reduction of nitro compounds has attracted increasing attention as it holds great promise for providing an alternative to the conventional synthetic process [17, 18, 39-47]. The required mild conditions and the possibility to decrease the generation of undesired products highlight its potential as a promising and green technique for selective reduction of nitro compounds to corresponding amines. Through a literature survey, it can be found that the investigation of magnetic based photocatalysts for photocatalytic selective organic transformation is very limited. In this paper, the magnetically separable  $\text{Fe}_3\text{O}_4/\text{SiO}_2/\text{CdS}$  photocatalysts were prepared *via* a simple method, using direct loaded CdS on the surface of silica-coated  $\text{Fe}_3\text{O}_4$  nanoparticles ( $\text{Fe}_3\text{O}_4/\text{SiO}_2$  core/shell) to develop novel methods for the photocatalytic reduction of nitro compounds [48-52]. The prepared nanocomposites were firstly employed as effective and magnetically recyclable photocatalysts in the reduction of aromatic nitro compounds to their corresponding amines under the blue LED irradiation in a very simple condition. The results showed that  $\text{Fe}_3\text{O}_4/\text{SiO}_2/\text{CdS}$  nanocomposites exhibited higher photocatalytic activity than bare CdS and commercial CdS (Aldrich).

## 2. Experimental Section:

### 2.1. Materials

Chemicals and apparatus:  $\text{FeCl}_3 \cdot 6\text{H}_2\text{O}$ ,  $\text{FeCl}_2 \cdot 4\text{H}_2\text{O}$ , cadmium acetate, 3-(mercaptopropyl) trimethoxysilane (MPTMS), and tetraethyl orthosilicate (TEOS) were purchased from Aldrich Co. Ammonia solution (25%), thiourea, toluene, dimethylformamide (DMF), and acetone were purchased from Merck Co. All reagents were used without further purification. Deionized water was used in all experiments.

### 2.2. Preparation of $\text{Fe}_3\text{O}_4/\text{SiO}_2/\text{CdS}$ nanocomposites:

Synthesis of  $\text{Fe}_3\text{O}_4$  nanoparticles: In order to prepare  $\text{Fe}_3\text{O}_4$  nanoparticles after mixing  $\text{FeCl}_2 \cdot 4\text{H}_2\text{O}$  (5.4 g) and  $\text{FeCl}_3 \cdot 6\text{H}_2\text{O}$  (2 g) in 2 M hydrochloric acid (25 mL) solution, ammonia solution [25% (v/v), 40 mL] was added dropwise over a period of 30 minutes under vigorous stirring. During the reaction, argon gas was allowed to flow through the flask. The magnetic nanoparticles were rinsed with deionized water ( $3 \times 30$  mL) and dried at 60 °C for 12 h in a vacuum oven [53].

Synthesis of  $\text{Fe}_3\text{O}_4/\text{SiO}_2$  nanoparticles: In order to prepare silica coated magnetic cores  $\text{Fe}_3\text{O}_4/\text{SiO}_2$  nanoparticles, 2 g of nanosized  $\text{Fe}_3\text{O}_4$  nanoparticles were dispersed in 50 mL of EtOH and 10 mL deionized water and sonicated for 15 min. 1.5 mL tetraethylorthosilicate (TEOS) was added dropwise and the mixture was sonicated for 10 min. Then 1 mL of ammonia solution [25% (v/v)] was added dropwise during 10 min. The hydrolysis of TEOS under alkaline condition was carried out in an ultrasonic bath for 3 h and the mixture was left to stand overnight. The silica coated particles were separated using an external magnet, washed three times with ethanol, and dried in a vacuum oven at 60 °C for 12 h [54].

Synthesis of thiolated magnetic nanoparticles: In a typical procedure, 2 mL of 3-(mercaptopropyl) trimethoxysilane (MPTMS) was added to 40 mL of a toluene suspension containing 2 g of  $\text{Fe}_3\text{O}_4/\text{SiO}_2$  nanoparticles. The mixture was refluxed for 24 h under constant stirring. The product  $\text{Fe}_3\text{O}_4\text{-SiO}_2\text{PrSH}$  (TMNP) was separated by external magnet, washed with EtOH, and dried in a vacuum oven at 45 °C for 12 h.

Synthesis of  $\text{Fe}_3\text{O}_4/\text{SiO}_2/\text{CdS}$  nanocomposites: The obtained thiopropyl-coated nanomagnets (TMNP) were subjected to supporting CdS. 200 mg of TMNP was added to 25 ml of DMF solution, containing different amounts of cadmium acetate and thiourea (The amount of cadmium acetate : thiourea were 1:1.82, 2:3.75, 4:7.5 mmol). Then the reaction mixture was exposed to ultrasound for 15 min followed by heating at 135 °C for 15 min. The resulting brownish solids were magnetically separated, washed with EtOH three consecutive times, and dried in an oven at 45 °C for 12 h. (Figure 1) The products obtained with different amounts of cadmium acetate 1, 2, and 4 mmol were named as S1, S2, and S4 respectively, while  $\text{Fe}_3\text{O}_4/\text{SiO}_2$  was labeled as S0.

Synthesis of bare CdS: 25 mL of a DMF solution containing cadmium acetate (2 mmol) and thiourea (3.75 mmol) were heated at 135 °C for 15 min. The resulting yellow solids were filtered and washed with EtOH three consecutive times and dried in an oven at 45 °C for 12 h.

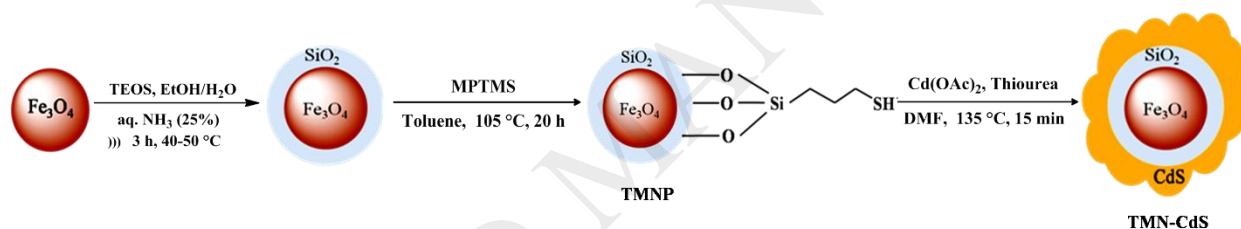


Figure 1. Illustration of the preparation of  $\text{Fe}_3\text{O}_4/\text{SiO}_2/\text{CdS}$  nanocomposites

The prepared samples were characterized by X-ray diffraction (XRD), Fourier transform infrared spectroscopy (FT-IR), transmission electron microscopy (TEM), UV-Vis spectroscopy, energy dispersive X-ray (EDX), and UV-Vis diffuse reflectance spectroscopy (DRS). Magnetic properties of the prepared samples were investigated using a vibrating sample magnetometer (VSM) with an applied field between 10000 and 10000 Oe at room temperature.

### 2.3. Photocatalytic activity:

The  $\text{Fe}_3\text{O}_4/\text{SiO}_2/\text{CdS}$  (S2) with average amount of CdS has been chosen as a photocatalyst for the photocatalytic reduction of nitro compounds under the blue LED irradiation. In a 10 mL flask, 5 ml of 0.01 M nitro compounds solution and 0.02 g photocatalyst were charged. Then the flask was charged with pure argon. The resulting mixture was stirred for 20 h under LED irradiation. After this time, the catalyst was simply separated by employing an external

magnetic field and the remaining solution was analyzed using thin-layered chromatography (TLC) and Varian gas chromatograph (CP-3800). The conversion of nitro substrate, yield of amine, and selectivity for amine were defined as follows:

$$\text{Conversion (\%)} = (C_0 - C_{\text{nitro}}) / C_0 \times 100$$

$$\text{Yield (\%)} = C_{\text{amine}} / C_0 \times 100$$

$$\text{Selectivity (\%)} = C_{\text{amine}} / (C_0 - C_{\text{nitro}}) \times 100$$

Where  $C_0$  is the initial concentration of nitro compound and  $C_{\text{nitro}}$  and  $C_{\text{amine}}$  are the concentration of the nitro substrate and the corresponding amine respectively, after the photocatalytic reaction.

### 3. Result and discussion:

In order to prepare the photocatalysts, a known silica-coated nanomagnet was chosen, which can be easily prepared from cheap starting materials according to the reported procedure with little modification [53, 54]. The resulting  $\text{Fe}_3\text{O}_4/\text{SiO}_2$  nanoparticles were then allowed to react under vigorous stirring with an appropriate concentration of (3-mercaptopropyl) trimethoxysilane to give thiol-functionalized silica-coated nanomagnets ( $\text{Fe}_3\text{O}_4/\text{SiO}_2/\text{PrSH}$ ). To this end, the obtained thiolpropyl-coated nanomagnets were subjected to react with cadmium acetate and thiourea to form the  $\text{Fe}_3\text{O}_4/\text{SiO}_2/\text{CdS}$  nanocomposites (TMN-CdS) (Figure 1).

The crystal structure of the prepared materials was characterized using XRD pattern and TEM images. The diffraction patterns of the prepared  $\text{Fe}_3\text{O}_4/\text{SiO}_2/\text{CdS}$  nanocomposites are similar and in good agreement with cubic phase of CdS. The XRD patterns of TMNP,  $\text{Fe}_3\text{O}_4/\text{SiO}_2/\text{CdS}$  nanocomposites, and bare CdS are shown in Figure 2. All the diffraction peaks can be indexed to the  $\text{Fe}_3\text{O}_4$  (JCPDS card no.; 75-1609) and cubic phase CdS (JCPDS card no. 10-0454) [14].

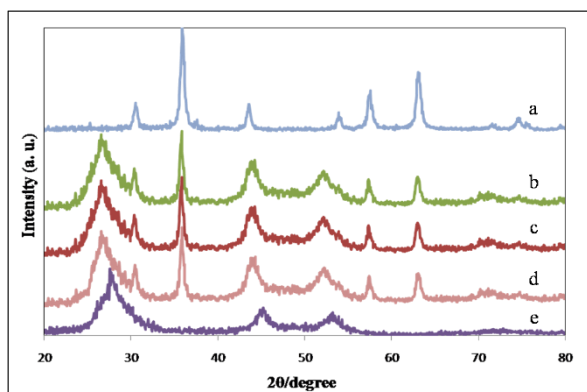


Figure 2. X-ray powder diffraction patterns of (a) TMNP, (b) S4, (c) S2, (d) S1, and (e) bare CdS

The morphology of the  $\text{Fe}_3\text{O}_4/\text{SiO}_2/\text{CdS}$  nanocomposites was examined by SEM. An overview of the images for the prepared samples demonstrates that the product consists of small nanostructures. The SEM image of TMN-CdS (S2) is shown in Figure 3a. The TEM image of the same sample (Figure 3b) indicates that the average size of the nanostructures is less than 40 nm. The energy dispersive X-ray spectroscopy (EDX) analysis of TMN-CdS nanocomposites confirmed the presence of the elements Cd, S, Fe, and Si (Figure 4). Additionally, the EDX results indicate that the wt % of Cd and S increased by increasing the amount of CdS precursors. The FT-IR spectrum of the prepared samples showed peaks that are characteristic of  $\text{Fe}_3\text{O}_4/\text{SiO}_2/\text{CdS}$  nanocomposites, which clearly differ from those of the unfunctionalized silica coated nanomagnets and thiol functionalized magnetic nanoparticles. This analysis, in combination with XRD and EDX data, indicated the successful anchoring of the CdS particles on the surface of magnetic nanoparticles.

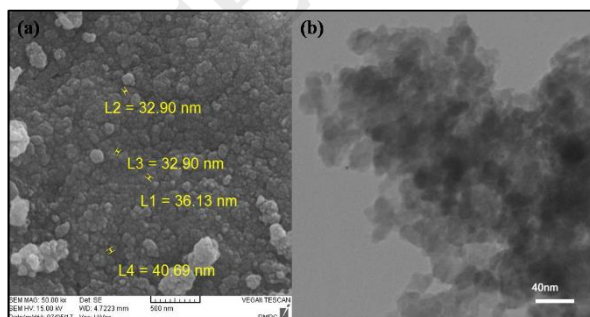


Figure 3. SEM (a) and TEM (b) images of  $\text{Fe}_3\text{O}_4/\text{SiO}_2/\text{CdS}$  nanocomposites (S2)

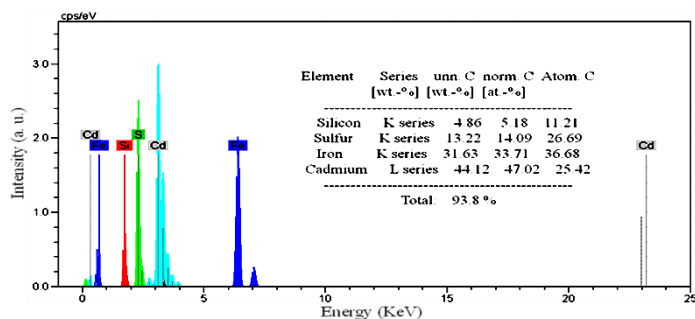


Figure 4. EDX spectrum of the  $\text{Fe}_3\text{O}_4/\text{SiO}_2/\text{CdS}$  nanocomposites (S2)

The ultraviolet-visible (UV-Vis) and diffuse reflectance spectra (DRS) were used to determine the optical properties of the samples (Figure 5). The UV-Vis spectra showed extended absorption within the visible light range compared with bare CdS. The enhanced absorption capability of visible light of  $\text{Fe}_3\text{O}_4/\text{SiO}_2/\text{CdS}$  nanocomposites suggests that it might have the higher photocatalytic activity for target reactions under visible light irradiation. A plot obtained via the transformation based on Kubelka-Munk function versus the energy of light is shown in (Figure 5b and 5c). As the amount of CdS precursors increased, the amount of band gap decreased as a result of the increase in particles size.

The BET specific surface area of the samples was calculated for  $\text{N}_2$  isotherm and was found to be about 103.25, 23.65, 11.26, and  $10.92\text{m}^2/\text{g}$  for S0, S1, S2, and S4. These results showed that growing CdS particles on the surface of  $\text{Fe}_3\text{O}_4/\text{SiO}_2$  nanoparticles led to a decreased BET surface area.

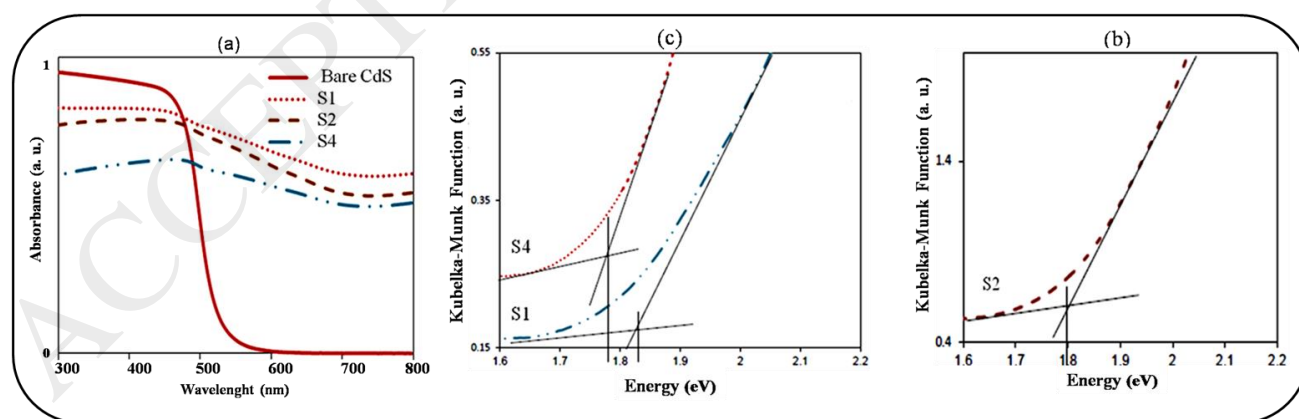


Figure 5. (a) UV-Vis diffuse reflectance spectra (DRS) of the bare CdS and  $\text{Fe}_3\text{O}_4/\text{SiO}_2/\text{CdS}$  nanocomposites (S1, S2, and S4), (b, c) the plot of transformed Kubelka-Munk function versus the energy of light

Magnetic measurements were investigated using VSM at room temperature in the applied magnetic field sweeping from -10 to 10 kOe (Figure 6). The saturation magnetization of these magnetic nanoparticles was between 20-18 emu/g. The decrease in  $M_s$  is attributed to the increased mass of CdS nanoparticles. Good magnetic properties imply strong magnetic responsivity of  $\text{Fe}_3\text{O}_4/\text{SiO}_2/\text{CdS}$ , which enable them to be separated easily.

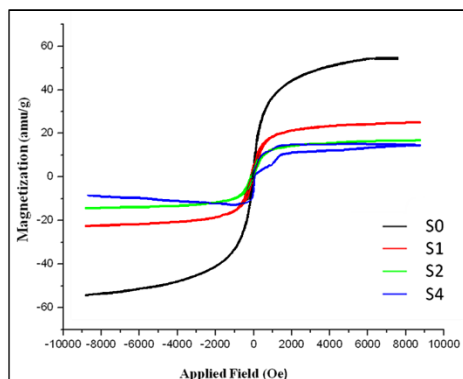


Figure 6. Room temperature magnetization curve of  $\text{Fe}_3\text{O}_4/\text{SiO}_2$  (S0) and  $\text{Fe}_3\text{O}_4/\text{SiO}_2/\text{CdS}$  nanocomposites (S1, S2, and S4)

Quantitative weight fraction of CdS in each sample was calculated based on atomic absorption spectrometer. The results show that the weight fraction of CdS in the sample increases by increasing the amount of CdS precursors. More specifically, it is 40%, 54%, and 60% in samples S1, S2, and S4, respectively.

In a series of further experiments, it was found that as the amount of CdS precursors increased, the CdS formation was not only led on the surface of MNPs and the CdS particles tended to rapidly aggregate in a random manner. Additionally, in this condition, the magnetic properties of nanocomposites decreased and good separation was not achieved by external magnet.

The photocatalytic activity of  $\text{Fe}_3\text{O}_4/\text{SiO}_2/\text{CdS}$  nanocomposite (S2) was examined in the photocatalytic reduction of nitrobenzene under the blue LED irradiation. According to the DRS spectra, the maximum absorption of the synthesized samples was near the wavelengths distribution of the blue LED [55]. Therefore, the blue LED was selected as a light source to examine the photocatalytic activity of the photocatalyst. In addition, using LED lamps as a light source is associated with several advantages such as high photon efficiency, low voltage electrical power source, power stability, emission in broader spectral wavelength, and no need for cooling during long time operation for complete photocatalytic reactions [56-58].

In order to determine optimal experimental condition, the reduction of nitrobenzene was subjected to a series of experimental conditions: first, the impact of various solvents such as EtOH and *i*-PrOH were examined.

Table 1. Optimization of the photocatalytic reduction condition of nitro benzene with Fe<sub>3</sub>O<sub>4</sub>/SiO<sub>2</sub>/CdS nanocomposites (S2) under blue LED (3 W) irradiation and argon atmosphere, irradiation time: 20 h.

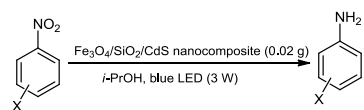
Entry	Nitrobenzene (M)	Solvent	Fe <sub>3</sub> O <sub>4</sub> /SiO <sub>2</sub> /CdS (mg)	Aniline <sup>a</sup> (%)	Conversion <sup>a</sup> (%)	Selectivity (%)
1	0.01	EtOH	20	7	98	7
2	0.01	<i>i</i> -PrOH	20	43	48	90
3	0.01	<i>i</i> -PrOH	40	36	100	36
4	0.01	<i>i</i> -PrOH	10	25	30	25
5	0.001	<i>i</i> -PrOH	20	12	100	12
6 <sup>b</sup>	0.01	<i>i</i> -PrOH	100	0	0	0
7	0.01	<i>i</i> -PrOH	0	0	0	0
8 <sup>c</sup>	0.01	<i>i</i> -PrOH	20	0	0	0

<sup>a</sup> Determined by gas chromatography.

<sup>b</sup> In the dark.

<sup>c</sup> Under air atmosphere.

It was found that *i*-PrOH was better as a reaction solvent for this photocatalytic reaction (Table 1, entries 1 and 2). In the presence of EtOH, the low selectivity of amine was observed. Notably, increasing the amount of photocatalyst from 10 to 20 mg resulted in higher yields, but increasing the amount of photocatalyst to 40 mg did not produce significant higher yields than the 20 mg of the photocatalyst (Table 1, entries 2-4). It was also noted that the reduction of nitrobenzene was not observed neither without Fe<sub>3</sub>O<sub>4</sub>/SiO<sub>2</sub>/CdS under LED irradiation nor using the Fe<sub>3</sub>O<sub>4</sub>/SiO<sub>2</sub>/CdS without LED irradiation (Table 1, entries 6 and 7). In addition, photocatalytic activity was observed only in argon atmosphere (Table 1, entry 8). Other optimum results are illustrated in Table 1. With optimal reaction conditions for the photocatalytic reduction of nitrobenzene under blue LED irradiation, the scope of this new photocatalytic reduction protocol was then investigated for other aromatic nitro compounds. As shown in Table 2, various types of aromatic nitro compound, including those with both electron-withdrawing and electron-donating groups, were converted to the corresponding amines in good yields under the optimal reaction conditions. These results show that electronic effects have significant effect on the products yields. Electron-deficient nitrobenzene derivatives have higher yields in this reaction condition due to their higher reduction potential.

Table 2. Photocatalytic reduction of nitrobenzene derivatives to corresponding amines via Fe<sub>3</sub>O<sub>4</sub>/SiO<sub>2</sub>/CdS nanocomposite (S2).<sup>a</sup>

Entry	Starting material	Amine	Yield (%) <sup>b, c</sup>	Conversion (%) <sup>b, c</sup>	Selectivity <sup>c</sup>
1			95(94)	100(100)	95(94)
2			98(96)	100(98)	98(98)
3			94(93)	100(100)	94(93)
4			40(18)	50(25)	80(72)
5			100(81)	100(82)	100(98)
6			43(2)	52(3)	83(66)
7			30(4)	79(5)	40(80)
8			80(15)	100(17)	80(88)
9			60(3)	100(7)	60(42)
10			60(2)	90(64)	67(31)
11			63(3)	100(5)	63(60)
12			55(6)	65(8)	85(75)
13 <sup>d</sup>			19	21	90

<sup>a</sup> Photocatalyst: 20 mg; nitro compound alcoholic solution ( $1 \times 10^{-2}$ M) 5 mL; blue LED irradiation (3 W) 80 Lumen; irradiation time: 20 h.

<sup>b</sup> Determined by gas chromatography.

<sup>c</sup> Numbers in parentheses represent results in the presence of 20 mg of the bare CdS.

<sup>d</sup> In the presence of commercial CdS (Aldrich).

$\text{Fe}_3\text{O}_4/\text{SiO}_2/\text{CdS}$  nanocomposite exhibited a much higher activity than bare CdS (Table 2). The photoirradiation of CdS photocatalysts leads to optical excitation across the band gap resulting in charge separation within the particles, that is, the excitation of electrons into the conduction band and the accompanying hole generation in the valence band under visible light irradiation. The high efficiency of  $\text{Fe}_3\text{O}_4/\text{SiO}_2/\text{CdS}$  nanocomposites as a photocatalyst is attributed to a large driving force for electron transfer from CdS to nitro compounds. The reduction potential of aromatic nitro compounds has been reported between  $-0.59$  and  $-0.25$  V vs NHE [59] and suitable levels of CdS conduction band (CB:  $-0.75$  V vs NHE) [60] clearly recognized the thermodynamic aspect of electrons realizing from CdS conduction band to the aromatic nitro compounds. In addition, the silica core as a photochemically inactive support exerts a positive influence on the reaction rate through including selective substrate adsorption, providing stability of nano sized CdS, and effective prevention of CdS agglomeration [61, 62]. As a result, the adsorbed nitro compounds on silica surface can be effectively reduced to their corresponding amines by accepting photocatalytic generated electrons (Figure 7). The photoactivity of  $\text{Fe}_3\text{O}_4/\text{SiO}_2/\text{CdS}$  nanocomposites in the photoreduction of nitrobenzene was also compared with that of commercial CdS (Aldrich) as a typically available photocatalyst. Commercial CdS tended to agglomerate to the size of more than 100 nm [52]. It was observed that the synthesized  $\text{Fe}_3\text{O}_4/\text{SiO}_2/\text{CdS}$  nanocomposites are more efficient than commercial CdS (Aldrich) (Table 2, entries 13).

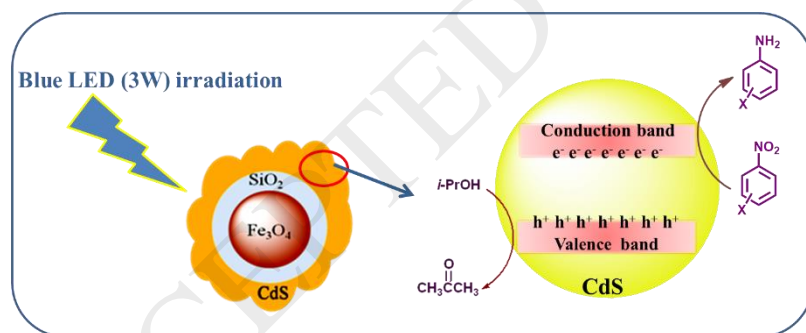


Figure 7. Photocatalytic reduction of nitro compounds in the presence of  $\text{Fe}_3\text{O}_4/\text{SiO}_2/\text{CdS}$  nanocomposites

To study the reusability and stability of the  $\text{Fe}_3\text{O}_4/\text{SiO}_2/\text{CdS}$  nanocomposites, the photocatalytic reduction of 3-nitroacetophenone was repeated for five times with the same photocatalyst (Figure 8). After each run, the photocatalyst was separated by external magnet and washed with *i*-PrOH, then used again in the photocatalytic reduction of nitrocompound. The little decrease observed after each run can be attributed to the loss of  $\text{Fe}_3\text{O}_4/\text{SiO}_2/\text{CdS}$

nanocomposites during washing and separating steps. In addition, some CdS particles were detached from the Fe<sub>3</sub>O<sub>4</sub>/SiO<sub>2</sub> core/shell surface during the recycling of the photocatalyst. However, the amount of Cd<sup>2+</sup> is detected before and after each reaction (runs 1–5) by atomic absorption spectroscopy (AAS) (which was 0.9 and 2.1, 2.3, 3.7, 4.1, and 4.2 ppm respectively), demonstrating the negligible detaching of CdS from the surface of the photocatalyst. This indicates that the Fe<sub>3</sub>O<sub>4</sub>/SiO<sub>2</sub>/CdS catalysts are fairly stable and possess the potential for practical application.

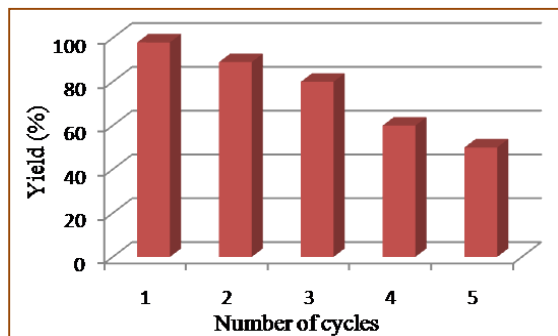


Figure 8. Representation of 3-amino acetophenone yields at different reuses of the photocatalyst

#### 4. Conclusions

In conclusion, magnetic Fe<sub>3</sub>O<sub>4</sub>/SiO<sub>2</sub>/CdS nanocomposites were synthesized through a facile and convenient method. The photocatalytic performance of the as-prepared photocatalysts was examined by the reduction of a wide range of aromatic nitro compounds under visible LED irradiation. The Fe<sub>3</sub>O<sub>4</sub>/SiO<sub>2</sub>/CdS nanocomposites exhibited enhanced photoactivity as compared with bare CdS and commercial CdS (Aldrich). This system couples the advantages of LED irradiation with low electrical power as a visible light source and easy separation and reusability of the photocatalyst, which makes it as a promising photocatalyst for other organic transformations.

#### Acknowledgments

The authors gratefully acknowledge the support provided by the Institute for Advanced Studies in Basic Sciences (IASBS).

## References

1. M.R. Hoffmann, S.T. Martin, W. Choi, D.W. Bahnemann, Environmental applications of semiconductor photocatalysis, *Chem. Rev.* 95 (1995) 69-96.
2. P.V. Kamat, Meeting the clean energy demand: nanostructure architectures for solar energy conversion, *J. Phys. Chem. C* 111 (2007) 2834-2860.
3. X. Chen, S.S. Mao, Titanium dioxide nanomaterials: synthesis, properties, modifications, and applications, *Chem. Rev.* 107 (2007) 2891-2959.
4. N. Zhang, S.J. Xie, B. Weng, Y.J. Xu, Vertically aligned ZnO-au@CdS core-shell nanorod arrays as an all-solid-state vectorial Z-scheme system for photocatalytic application, *J. Mater. Chem. A* 4 (2016) 18804–18814.
5. X. Liu, Y. Qin, Y. Yan, P. Lv, The fabrication of CdS/CoFe<sub>2</sub>O<sub>4</sub>/rGO photocatalysts to improve the photocatalytic degradation performance under visible light, *RSC Adv.* 7 (2017) 40673-40681.
6. L. Chen, W. Ma, J. Dai, J. Zhao, C. Li, Y. Yan, Facile synthesis of highly efficient graphitic-C<sub>3</sub>N<sub>4</sub>/ZnFe<sub>2</sub>O<sub>4</sub> heterostructures enhanced visible-light photocatalysis for spiramycin degradation, *J. Photochem. Photobiol. A* 328 (2016) 24-32.
7. D. Jing, L. Guo, A novel method for the preparation of a highly stable and active CdS photocatalyst with a special surface nanostructure, *J. Phys. Chem. B* 110 (2006) 11139-11145.
8. P. Kumar, P.K. Singh, B. Bhattacharya, Study of nano-CdS prepared in methanolic solution and polymer electrolyte matrix, *Ionics* 17 (2011) 721-725.
9. J. Britt, C. Ferekides, Thin-film CdS/CdTe solar cell with 15.8% efficiency, *Appl. Phys. Lett.* 62 (1993) 2851-2852.
10. J. Chu, Z. Jin, W. Wang, H. Liu, D. Wang, J. Yang, Z. Hong, Influence of anionic concentration and deposition temperature on formation of wurtzite CdS thin films by in situ chemical reaction method, *J. Alloys Compd.* 517 (2012) 54-60.
11. S. Chun, Y. Jung, J. Kim, D. Kim, The analysis of CdS thin film at the processes of manufacturing CdS/CdTe solar cells, *J. Cryst. Growth* 326 (2011) 152-156.
12. L.Y. Wang, L. Wang, F. Gao, Z.Y. Yu, Z.M. Wu, Application of functionalized CdS nanoparticles as fluorescence probe in the determination of nucleic acids, *Analyst* 127 (2002) 977-980.
13. R.M. Ma, L. Dai, H.B. Huo, W.J. Xu, G. Qin, High-performance logic circuits constructed on single CdS nanowires, *Nano Lett.* 7 (2007) 3300-3304.

14. X. Liu, Z. Fang, X. Zhang, W. Zhang, X. Wei, B. Geng, Preparation and characterization of Fe<sub>3</sub>O<sub>4</sub>/CdS nanocomposites and their use as recyclable photocatalysts, *Cryst. Growth Des.* 9 (2008) 197-202.
15. G.R. Andrade, C.C. Nascimento, E.C. Neves, C.D. Barbosa, L.P. Costa, L.S. Barreto, I.F. Gimenez, One-step preparation of CdS nanocrystals supported on thiolated silica-gel matrix and evaluation of photocatalytic performance, *J. Hazard. Mater.* 203 (2012) 151-157.
16. Y. Liu, L. Zhou, Y. Hu, C. Guo, H. Qian, F. Zhang, X.W.D. Lou, Magnetic-field induced formation of 1D Fe<sub>3</sub>O<sub>4</sub>/C/CdS coaxial nanochains as highly efficient and reusable photocatalysts for water treatment, *J. Mater. Chem.* 21 (2011) 18359-18364.
17. B. Weng, S. Liu, N. Zhang, Z.R. Tang, Y.J. Xu, A simple yet efficient visible-light-driven CdS nanowires-carbon nanotube 1D–1D nanocomposite photocatalyst, *J. Catal.* 309 (2014) 146–155.
18. N. Zhang, M.Q. Yang, S. Liu, Y. Sun, Y.J. Xu, Waltzing with the Versatile Platform of Graphene to Synthesize Composite Photocatalysts, *Chem. Rev.* 115 (2015) 10307–10377.
19. Z. Chen, S. Liu, M.Q. Yang, Y.J. Xu, Synthesis of uniform CdS nanospheres/graphene hybrid nanocomposites and their application as visible light photocatalyst for selective reduction of nitro organics in water, *ACS Appl. Mater. Interfaces* 5 (2013) 4309-4319.
20. Z. Gao, N. Liu, D. Wu, W. Tao, F. Xu, K. Jiang, Graphene–CdS composite, synthesis and enhanced photocatalytic activity, *Appl. Surf. Sci.* 258 (2012) 2473-2478.
21. C. Nethravathi, T. Nisha, N. Ravishankar, C. Shivakumara, M. Rajamathi, Graphene–nanocrystalline metal sulphide composites produced by a one-pot reaction starting from graphite oxide, *Carbon* 47 (2009) 2054-2059.
22. E. Caponetti, L. Pedone, M. Saladino, D. Chillura Martino, G. Nasillo, MCM-41-CdS nanoparticle composite material: preparation and characterization, *Microporous Mesoporous Mater.* 128 (2010) 101-107.
23. X. Du, J. He, Elaborate control over the morphology and structure of mercapto-functionalized mesoporous silicas as multipurpose carriers, *Dalton Trans.* 39 (2010) 9063-9072.
24. S. Watson, D. Beydoun, R. Amal, Synthesis of a novel magnetic photocatalyst by direct deposition of nanosized TiO<sub>2</sub> crystals onto a magnetic core, *J. Photochem. Photobiol. A* 148 (2002) 303-313.
25. X.W. Lou, L.A. Archer, A general route to nonspherical anatase TiO<sub>2</sub> hollow colloids and magnetic multifunctional particles, *Adv. Mater.* 20 (2008) 1853-1858.

26. W. Wu, C. Jiang, V.A.L. Roy, Recent progress in magnetic iron oxide–semiconductor composite nanomaterials as promising photocatalysts, *Nanoscale* 7 (2015) 38–58.
27. W. Jiang, C. Jiang, Z. Cao, X. Gong, Z. Zhang, Fabrication and characterization of photocatalytic activity of Fe<sub>3</sub>O<sub>4</sub> doped CdS hollow spheres, *J. Phys. Chem. Solids* 70 (2009) 782-786.
28. H. Yao, M. Fan, Y. Wang, G. Luo, W. Fei, Magnetic titanium dioxide based nanomaterials: synthesis, characteristics, and photocatalytic application in pollutant degradation, *J. Mater. Chem. A* 3 (2015)17511-17544.
29. J.W. Xu, Z.D. Gao, K. Han, Y. Liu, Y.Y. Song, Synthesis of magnetically separable Ag<sub>3</sub>PO<sub>4</sub>/TiO<sub>2</sub>/Fe<sub>3</sub>O<sub>4</sub> heterostructure with enhanced photocatalytic performance under visible light for photoinactivation of bacteria, *ACS Appl. Mater. Interfaces* 6 (2014) 15122-15131.
30. R. Chalasani, S. Vasudevan, Cyclodextrin-functionalized Fe<sub>3</sub>O<sub>4</sub>@TiO<sub>2</sub>: reusable, magnetic nanoparticles for photocatalytic degradation of endocrine-disrupting chemicals in water supplies, *ACS Nano* 7 (2013) 4093-4104.
31. Y. Wang, F. Pan, W. Dong, L. Xu, K. Wu, G. Xu, W. Chen, Recyclable silver-decorated magnetic Titania nanocomposite with enhanced visible-light photocatalytic activity, *Appl. Catal. B Environ.* 189 (2016) 192-198.
32. Y. Tang, G. Zhang, C. Liu, S. Luo, X. Xu, L. Chen, B. Wang, Magnetic TiO<sub>2</sub>-graphene composite as a high-performance and recyclable platform for efficient photocatalytic removal of herbicides from water, *J. Hazard. Mater.* 252–253 (2013) 115-122.
33. Z. Zhu, X. Tang, S. Kang, P. Huo, M. Song, W. Shi, Z. Lu, Y. Yan, Constructing of the magnetic photocatalytic nanoreactor MS@FCN for cascade catalytic degrading of tetracycline, *J. Phys. Chem. C* 120 (2016) 27250–27258.
34. Z. Zhua, Y. Yua, H. Huang, X. Yao, H. Dong, Z. Liub, Y. Yana, C. Lia, P. Huoa, Microwave-hydrothermal synthesis of a novel recyclability, stability photocatalytic nanoreactor for orienting recognition and degrading of tetracycline, *Catal. Sci. Technol.* 7 (2017) 4092-4104.
35. Z. Zhu, Y. Yu, H. Dong, Z. Liu, C. Li, P. Huo, Y. Yan, Intercalation effect of ATP in g-C<sub>3</sub>N<sub>4</sub> modified with Fe<sub>3</sub>O<sub>4</sub>-QDs to enhance photocatalytic activity for removing 2-Mercaptobenzothiazole under visible light, *ACS Sustainable Chem. Eng.* 5 (2017) 10614–10623.
36. A. Truppi, F. Petronella, T. Placido, M. Striccoli, A. Agostiano, M.L. Curri, R. Comparelli, Visible-light-active. TiO<sub>2</sub>-based hybrid nanocatalysts for environmental applications, *Catalysts* 7 (2017) 100-133.
37. Z. Zhu, W. Fan, Z. Liu, H. Dong, Y. Yan, P. Huo, Construction of an attapulgite intercalated mesoporous g-C<sub>3</sub>N<sub>4</sub> with enhanced photocatalytic activity for antibiotic degradation, *J. Photochem. Photobiol. A* 359 (2018) 102-110.

38. Z. Zhu, W. Fan, Z. Liu, Y. Yu, H. Dong, P. Huo, Y. Yan, Fabrication of the metal-free biochar-based graphitic carbon nitride for improved 2-Mercaptobenzothiazole degradation activity, *J. Photochem. Photobiol. A* 358 (2018) 284-293.
39. W. Wu, G. Liu, Q. Xie, S. Liang, H. Zheng, R. Yuan, W. Su, L. Wu, A simple and highly efficient route for the preparation of p-phenylenediamine by reducing 4-nitroaniline over commercial CdS visible light-driven photocatalyst in water, *Green Chem.* 14 (2012) 1705-1709.
40. S. Liu, Z. Chen, N. Zhang, Z.R. Tang, Y.J. Xu, An efficient self-assembly of CdS nanowires–reduced graphene oxide nanocomposites for selective reduction of nitro organics under visible light irradiation, *J. Phys. Chem. C* 117 (2013) 8251-8261.
41. A. Hernández-Gordillo, A.G. Romero, F. Tzompantzi, S. Oros-Ruiz, R. Gómez, Visible light photocatalytic reduction of 4-Nitrophenol using CdS in the presence of Na<sub>2</sub>SO<sub>3</sub>, *J. Photochem. Photobiol. A* 257 (2013) 44-49.
42. M.Q. Yang, N. Zhang, Y. Wang, Y.J. Xu, Metal-free, robust, and regenerable 3D graphene–organics aerogel with high and stable photosensitization efficiency, *J. Catal.* 346 (2017) 21–29.
43. M.S. Deenadayalan, N. Sharma, P.K. Verma, C.M. Nagaraja, Visible-light-assisted photocatalytic reduction of nitroaromatics by recyclable Ni(II)-porphyrin metal–organic framework (MOF) at RT, *Inorg. Chem.* 55 (2016) 5320-5327.
44. L. Zhang, X. He, X. Xu, C. Liu, Y. Duan, L. Hou, Q. Zhou, C. Ma, X. Yang, R. Liu, F. Yang, L. Cui, C. Xu, Y. Li, Highly active TiO<sub>2</sub>/g-C<sub>3</sub>N<sub>4</sub>/G photocatalyst with extended spectral response towards selective reduction, *Appl. Catal. B Environ.* 203 (2017) 1-8.
45. N. Zhang, M.Q. Yang, Z.R. Tang, Y.J. Xu, Toward improving the graphene-semiconductor composite photoactivity via the addition of metal ions as generic interfacial mediator. *ACS Nano* 8 (2014) 623–633.
46. W.Z. Gao, Y. Xu, Y. Chen, W.F. Fu, Highly efficient and selective photocatalytic reduction of nitroarenes using the Ni<sub>2</sub>P/CdS catalyst under visible-light irradiation, *Chem. Commun.* 51 (2015) 13217-13220.
47. S.K. Pahari, P. Pal, D.N. Srivastava, S.C. Ghosh, A.B. Panda, Efficient photocatalytic selective nitro-reduction and C–H bond oxidation over ultrathin sheet mediated CdS flowers, *Chem. Commun.* 51 (2015) 10322-10325.
48. P. Eskandari, F. Kazemi, Z. Zand, Photocatalytic reduction of aromatic nitro compounds using CdS nanostructure under blue LED irradiation, *J. Photochem. Photobiol. A* 274 (2014) 7-12.

49. M. A. Kakroudi, F. Kazemi, B. Kaboudin,  $\beta$ -Cyclodextrin–TiO<sub>2</sub>: Green nest for reduction of nitroaromatic compounds, *RSC Adv.* 4 (2014) 52762-52769.
50. Z. Zand, F. Kazemi, S. Hosseini, Development of chemoselective photoreduction of nitro compounds under solar light and blue LED irradiation, *Tetrahedron Lett.* 55 (2014) 338-341.
51. M. Ramdar, F. Kazemi, B. Kaboudin, Z. Taran, A. Partovi, Visible light active CdS nanorods: one-pot synthesis of aldonitrones, *New J. Chem.* 40 (2016) 9257-9262.
52. A.A. Safari, F. Kazemi, Photocatalytic reduction of nitro aromatic compounds to amines using a nanosized highly active CdS photocatalyst under sunlight and blue LED irradiation, *Chem. Pap.* 70 (2016) 531-537.
53. C.T. Chen, Y.C. Chen, Fe<sub>3</sub>O<sub>4</sub>/TiO<sub>2</sub> core/shell nanoparticles as affinity probes for the analysis of phosphopeptides using TiO<sub>2</sub> surface-assisted laser desorption/ionization mass spectrometry, *Anal. Chem.* 77 (2005) 5912-5919.
54. B. Karimi, E. Farhangi, A highly recyclable magnetic core-shell nanoparticle-supported TEMPO catalyst for efficient metal-and halogen-free aerobic oxidation of alcohols in water, *Chem. Eur. J.* 17 (2011) 6056-6060.
55. P. Eskandari, F. Kazemi, Y. Azizian, Convenient preparation of CdS nanostructures as a highly efficient photocatalyst under blue LED and solar light irradiation, *Sep. Pur. Technol.* 120 (2013) 180-185.
56. Y. Li, Y. Jiang, S. Peng, F. Jiang, Nitrogen-doped TiO<sub>2</sub> modified with NH<sub>4</sub>F for efficient photocatalytic degradation of formaldehyde under blue light-emitting diodes, *J. Hazard. Mater.* 182 (2010) 90-96.
57. X. Wang, T.T. Lim, Solvothermal synthesis of C–N codoped TiO<sub>2</sub> and photocatalytic evaluation for bisphenol A degradation using a visible-light irradiated LED photoreactor, *Appl. Catal., B* 100 (2010) 355-364.
58. R.J. Tayade, T.S. Natarajan, H.C. Bajaj, Photocatalytic degradation of methylene blue dye using ultraviolet light emitting diodes, *Ind. Eng. Chem. Res.* 48 (2009) 10262-10267.
59. M. Uchimiya, L. Gorb, O. Isayev, M.M. Qasim, J. Leszczynski, One-electron standard reduction potentials of nitroaromatic and cyclic nitramine explosives, *Environ. Pollut.* 158 (2010) 3048–3053.
60. H. Park, Y.K. Kim, W. Choi, Reversing CdS preparation order and its effects on photocatalytic hydrogen production of CdS/Pt-TiO<sub>2</sub> hybrids under visible light, *J. Phys. Chem. C* 115 (2011) 6141–6148.
61. H. Weiß, A. Fernandez, H. Kisch, Electronic semiconductor–support interaction—A novel effect in semiconductor photocatalysis, *Angew. Chem. Int. Ed.* 40 (2001) 3825-3827.

62. M. Hopfner, H. Weiß, D. Meissner, F.W. Heinemann, H. Kisch, Semiconductor photocatalysis type B: synthesis of unsaturated  $\alpha$ -amino esters from imines and olefins photocatalyzed by silica-supported cadmium sulfide, Photochem. Photobiol. Sci. 1 (2002) 696-703.

ACCEPTED MANUSCRIPT